Acta Oncologica

ISSN: 0284-186X (Print) 1651-226X (Online) Journal homepage: informahealthcare.com/journals/ionc20

Dose-volume histogram analysis for risk factors of radiation-induced rib fracture after hypofractionated proton beam therapy for hepatocellular carcinoma

Ayae Kanemoto, Masashi Mizumoto, Toshiyuki Okumura, Hideto Takahashi, Takayuki Hashimoto, Yoshiko Oshiro, Nobuyoshi Fukumitsu, Takashi Moritake, Koji Tsuboi, Takeji Sakae & Hideyuki Sakurai

Acta Oncologica, 2013; 52: 538–544

informa healthcare

ORIGINAL ARTICLE

Dose-volume histogram analysis for risk factors of radiation-induced rib fracture after hypofractionated proton beam therapy for hepatocellular carcinoma

AYAE KANEMOTO[1], MASASHI MIZUMOTO[1], TOSHIYUKI OKUMURA[1], HIDETO TAKAHASHI[2], TAKAYUKI HASHIMOTO[1], YOSHIKO OSHIRO[1], NOBUYOSHI FUKUMITSU[1], TAKASHI MORITAKE[1], KOJI TSUBOI[1], TAKEJI SAKAE[1] & HIDEYUKI SAKURAI[1]

[1]*Proton Medical Research Center and Department of Radiation Oncology, University of Tsukuba, Tsukuba, Ibaraki, Japan, and* [2]*Department of Epidemiology and Biostatistics, Faculty of Medicine, University of Tsukuba, Tsukuba, Ibaraki, Japan*

Abstract

Background. Radiation-induced rib fracture has been reported as a late complication after external radiotherapy to the chest. The purpose of this study was to clarify the characteristics and risk factors of rib fracture after hypofractionated proton beam therapy (PBT). *Material and methods.* The retrospective study comprised 67 patients with hepatocellular carcinoma who were treated using PBT of 66 Cobalt-Gray-equivalents [Gy (RBE)] in 10 fractions. We analyzed the patients' characteristics and determined dose-volume histograms (DVHs) for the irradiated ribs, and then estimated relationships between risk of fracture and several dose-volume parameters. An irradiated rib was defined to be any rib included in the area irradiated by PBT as determined by treatment-planning computed tomography. *Results.* Among the 67 patients, a total of 310 ribs were identified as irradiated ribs. Twenty-seven (8.7%) of the irradiated ribs developed fractures in 11 patients (16.4%). No significant relationships were seen between incidence of fracture and characteristics of patients, including sex, age, tumor size, tumor site, and follow-up period ($p \geq 0.05$). The results of receiver operating characteristic curve analysis using DVH parameters demonstrated that the largest area under the curve (AUC) was observed for the volume of rib receiving a biologically effective dose of more than 60 Gy_3 (RBE) (V60) [The equivalent dose in 2 Gy fractions (EQD2); 36 Gy_3] and the AUCs of V30 to V120 (EQD2; 18–72 Gy_3) and D_{max} to D_{10cm^3} were similar to that of V60. No significant relationships were seen for DVH parameters and intervals from PBT to incidence of fracture. *Conclusion.* DVH parameters are useful in predicting late adverse events of rib irradiation. This study identified that V60 was a most statistically significant parameter, and V30 to V120 and D_{max} to D_{10cm^3} were also significant and clinically useful for estimating the risk of rib fracture after hypofractionated PBT.

With improvements in the accuracy of radiation delivery and techniques for calculation of radiotherapy doses, precisely directed focal high-dose radiation treatments, such as hypofractionated stereotactic radiotherapy (SRT), are being used more frequently. Because SRT can deliver directed and precise high-dose irradiation, it can be used not only for brain tumors, but also for extracranial tumors [1,2]. However, the use of SRT for lung tumors has shown that the risk of radiation-induced rib fracture is higher for SRT than for conventional external radiotherapy [3–11]. This side effect adversely affects the quality of life (QOL) of cancer patients, as rib fracture commonly causes prolonged pain and long-term disability [12].

Proton beam therapy (PBT) for hepatocellular carcinoma (HCC) has resulted in good local control with low frequency of adverse effects [13–16]. Late complications that have been reported to date include bile duct stenosis, gastrointestinal inflammation/ulceration, pneumonitis, hepatic insufficiency, and rib fracture [14–18]. Based on its

Correspondence: A. Kanemoto, Proton Medical Research Center and Department of Radiation Oncology, University of Tsukuba, 1-1-1 Tennoudai, Tsukuba, Ibaraki 305-8575, Japan. Tel: +81 29 8537100. Fax: +81 29 8537102. E-mail: ayaek@pmrc.tsukuba.ac.jp

(Received 29 November 2011; accepted 28 July 2012)

ISSN 0284-186X print/ISSN 1651-226X online
DOI: 10.3109/0284186X.2012.718094

efficacy and what is currently known about the complications of PBT, hypofractionated PBT at 66 Cobalt-Gray-equivalents [Gy (RBE)] in 10 fractions is used at Tsukuba University Hospital to treat HCC that is not adjacent to the gastrointestinal tract or the porta hepatis. However, some of the patients treated this way have developed rib fractures. This side effect after PBT has not been examined in detail. We therefore performed a dosimetric analysis using dose-volume histograms (DVHs) to evaluate the characteristics and risk factors of HCC patients developing rib fractures after PBT.

Material and methods

Patients

From May 2002 to December 2007, a total of 67 patients (47 men, 20 women) with HCC were treated using PBT at 66 Gy (RBE) in 10 fractions as their primary radiotherapy at Tsukuba University Hospital. We evaluated these patients retrospectively. The median age at the time of treatment was 69 years (range, 26–85 years). The Eastern Cooperative Oncology Group (ECOG) performance status (PS) of these patients was as follows: 37 patients with PS = 0, 29 with PS = 1, and one with PS = 2. There were 38 patients with one tumor mass, 13 with two, 12 with three, and four had ≥ 4 masses. The median size of the tumor treated using PBT was 31 mm (range, 6–93 mm). Forty-two patients had received another therapy for HCC before PBT, including radiofrequency ablation (RFA) and transcatheter arterial chemoembolization (TACE), while 25 patients received PBT as the initial treatment.

Proton beam therapy

At our hospital, the following three treatment protocols are commonly used depending on the tumor location: 66 Gy (RBE) in 10 fractions, 72.6 Gy (RBE) in 22 fractions, or 74 Gy (RBE) in 37 fractions [15,16,19]. The protocol using 66 Gy (RBE) in 10 fractions is applied when the tumor is not adjacent to the gastrointestinal tract or porta hepatis. The photon equivalent dose was defined as the physical dose (Gy) $\times$ the relative biological effectiveness of the proton beam, which was assigned a value of 1.1 in this study [20]. The equivalent dose in conventional fractionation (2.0 Gy per fraction: EQD2) was calculated based on a linear quadratic equation [21], assuming α/β ratio of 10 Gy for tumor and 3 Gy for late responding tissue. The biologically effective dose (BED) of 66 Gy (RBE) calculated with an α/β ratio of 10 Gy was 110 Gy_{10} (RBE) (EQD2; 91 Gy_{10}), and the dose calculated with an α/β ratio of 3 Gy was 211 Gy_3 (RBE) (EQD2; 127 Gy_3).

The clinical target volume (CTV) encompassed the gross tumor volume with a 5- to 10-mm margin in all directions [15,16]. An additional 5-mm margin was included in the caudal axes to compensate for uncertainty due to respiration-induced hepatic movements. Two or three beams were used, and an additional margin of 5- to 10-mm was added to cover the entire CTV by enlarging the multileaf collimator and adjusting the range shifter. Proton beams of 155–250 MeV were generated using a synchrotron accelerator, and were delivered during the expiratory phase under a respiration-gated system [22].

The ribs to be irradiated by proton beams were contoured at the treatment planning computed tomography (CT).

Follow-up and evaluations

The patients were followed from May 2002 to January 2010. Follow-up examinations, including measuring levels of tumor markers and imaging, were performed at intervals of at least six months. Rib fractures were identified using imaging such as CT. At the end of follow-up, 29 patients were alive and 38 had died. Durations of follow-up periods for all patients, two-year survivors, and all patients alive at January 2010 were 6.7–81.1 months (median, 27.7 months; mean, 30.7 months), 24.1–81.1 months (median, 38.3 months; mean, 40.7 months), and 8.7–81.1 months (median, 30.3 months; mean, 34.0 months), respectively.

Statistical analysis

Rib fracture rates were estimated using the Kaplan-Meier method [23]. Characteristics of patients with and without rib fractures were analyzed. The t-test was used to evaluate differences in age, tumor size, and follow-up period. χ^2 distributions were determined to evaluate differences in sex and tumor site. Tumor site was classified according to the anatomical segment.

A DVH was calculated for each irradiated rib. An irradiated rib was defined as a rib in the area irradiated by PBT as determined by the treatment planning CT. A BED with α/β=3 Gy (BED_3) was used to determine the radiation dose for ribs [Gy_3 (RBE)] and EQD2 was also calculated based on a linear quadratic model, assuming α/β=3 Gy. EQD2 contained the RBE-factor of 1.1. Relationships were determined for the incidence of rib fracture and DVH parameters as follows: V1 = volume of rib receiving >1 Gy_3 (RBE) (EQD2; 0.5 Gy_3), V30 = volume receiving >30 Gy_3 (RBE) (EQD2; 18 Gy_3), V60 = volume receiving >60 Gy_3 (RBE) (EQD2; 36 Gy_3), V90 = volume receiving >90 Gy_3 (RBE) (EQD2; 54 Gy_3), V120 = volume receiving > 120 Gy_3 (RBE) (EQD2; 72 Gy_3), V150 = volume receiving >150 Gy_3 (RBE) (EQD2; 90 Gy_3), V180 = volume receiving >180 Gy_3 (RBE) (EQD2; 108 Gy_3), and V210 = volume receiving >210 Gy_3 (RBE) (EQD2; 126 Gy_3). Relationships were also determined for the incidence of rib fracture and the maximum dose (D_{max}) Gy_3 (RBE) for irradiated ribs, and doses received by irradiated rib volumes of 1-cm^3 (D_{1cm^3}), 2-cm^3 (D_{2cm^3}), 5-cm^3 (D_{5cm^3}), and 10-cm^3 (D_{10cm^3}). The value of these doses was shown using BED_3. Data analysis was performed using SPSS version 11.0 software (SPSS, Chicago, Illinois). Values of $p < 0.05$ were considered significant.

For factors identified as significant in univariate analysis, receiver operating characteristics (ROC) curves were used to determine the optimal DVH parameter and cut-off point for predicting rib fracture. The ROC curve was a plot of the true-positive rate (sensitivity) as a function of the false-positive rate (1-specificity) over a range of DVH parameters. Areas under the curve (AUCs) were determined and the optimal cut-off point for each ROC curve was chosen as the cut-off value at the minimal value for $[(1-\text{specificity})^2 + (1-\text{sensitivity})^2]$ [24]. The optimal cut-off point should provide the highest sensitivity and specificity. The correlation coefficients between DVH parameters were determined, and the crude fracture rates above and below the cut-off point were also determined. After determining the optimal DVH parameter, volume-response curves and dose-response curves were generated using logistic regression with maximum likelihood estimation.

Results

Frequency and times to rib fracture

During the follow-up period, radiation-induced rib fracture was seen after PBT in 11 (seven men, four women) of 67 patients (16.4%). Their median age was 69 years (range, 53–85 years). There were a total of 310 irradiated ribs. Of these 310 ribs, 27 ribs (8.7%) developed fractures by the end of the follow-up period. Among these 11 patients, the median number of fractured ribs was two (range, 1–5). Three patients had metachronous occurrences. Eight patients were asymptomatic, but the remaining three patients complained of chronic pain, and one patient also complained of thoracic deformity.

For all 67 patients, the median period from the end of PBT to initial radiation-induced rib fracture or the end of follow-up was 25 months (range, 6.7–81 months). The five-year cumulative incidence was 22% (Figure 1a). For the 11 patients with fracture, the median period from the end of PBT to initial radiation-induced rib fracture was 15 months (range, 8.1–32 months). For all 310 irradiated ribs, the median period from the end of PBT to the identification of a fracture or the end of follow-up was 25 months (range, 6.7–67 months), and the five-year cumulative incidence was 13% (Figure 1b). For the 27 radiation-induced fractured ribs, the median period from the end of PBT to the identification of a fracture was 20 months (range, 8.1–32 months).

Characteristics of patients

The characteristics of patients with and without rib fracture were compared. No significant differences in factors such as sex, age, tumor size, tumor site, or

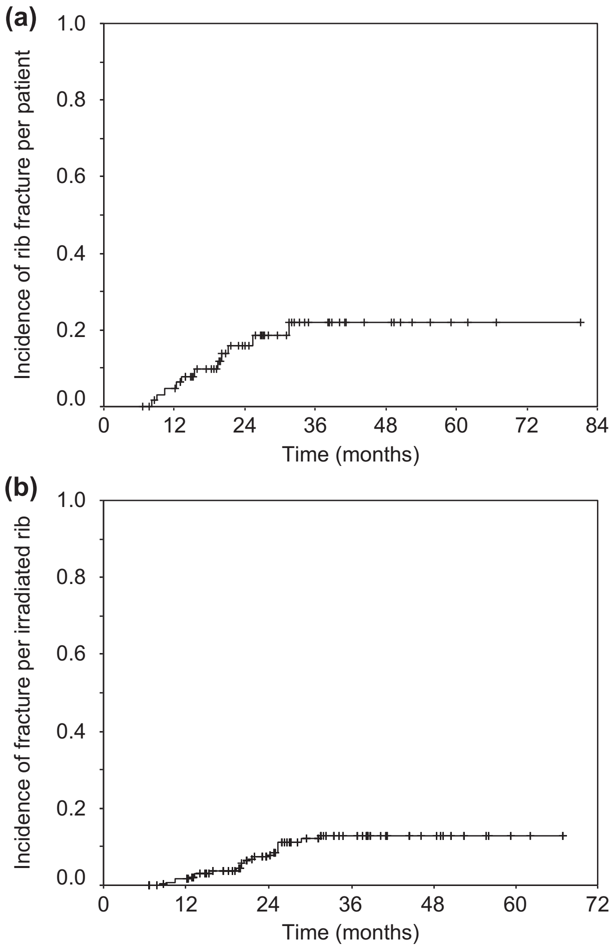

Figure 1. Time to rib fracture after hypofractionated proton beam therapy [proportion per patient (a) and proportion per irradiated rib (b)]. a) Among 67 patients, 11 (16.4%) developed rib fracture after proton beam therapy. The 5-year cumulative incidence of rib fracture was 22%. b) Among 310 irradiated ribs in all 67 patients, 27 ribs (8.7%) developed fracture, and the 5-year cumulative incidence of rib fracture was 13%.

follow-up period, were observed between these groups ($p \geq 0.05$).

DVH analysis of irradiated ribs

Relationships between radiation-induced rib fractures and volumes of irradiated ribs or doses to irradiated ribs were analyzed. Comparing volumes and doses, DVH parameters were all significantly higher in fractured ribs than in non-fractured ribs ($p < 0.05$) (Figure 2).

Relationship analysis of DVH parameters and the intervals from PBT to fracture was performed. No significant relationships were seen for volume parameters of all irradiated ribs and interval to fracture ($p \geq 0.05$). Relationships between doses to fractured ribs and interval times were not clearly significant ($p \geq 0.05$); however, the p-values for D_{max} to D_{2cm^3} were close to significant (D_{max}, $p = 0.052$; D_{1cm^3}, $p = 0.059$; D_{2cm^3}, $p = 0.059$), and the correlation coefficient of D_{max} was 0.378.

ROC analysis showed that the largest AUC was observed for V60, which AUC was 0.857 [95% confidence interval (CI) 0.791–0.923], and the AUCs of D_{max} and D_{1cm^3} were next largest. The correlation coefficient between V60 and D_{max} and that between V60 and D_{1cm^3} was 0.81 and 0.86, respectively. There was a relationship between DVH parameters, and the AUCs of V30 to V120 and D_{2cm^3} to D_{10cm^3} were also similar to that of V60. Each optimal cut-off point was statistically identified and the crude fracture rates above and below the cut-off point were also listed in Table I. The analysis of V60, which AUC was largest, showed an optimal cut-off point of 4.48 cm^3 (Figure 3a). The crude fracture rate was 1.4% (three fractured ribs / 219 ribs) when the volume of irradiated rib was <4.48 cm^3, and 26% (24 fractured ribs / 91 ribs) when the volume was ≥4.48 cm^3. The sensitivity and specificity of 4.48 cm^3 at V60 were 0.89 and 0.77, respectively. Curves of cumulative rates of fracture were significantly different between these two volumes according to the log-rank test ($p = 0.000$) (Figure 3b). In addition, the plots indicate that three years after radiation therapy, radiation-induced rib fractures should not occur.

Logistic regression was used to generate a volume-response curve of the fracture rate (p) as a

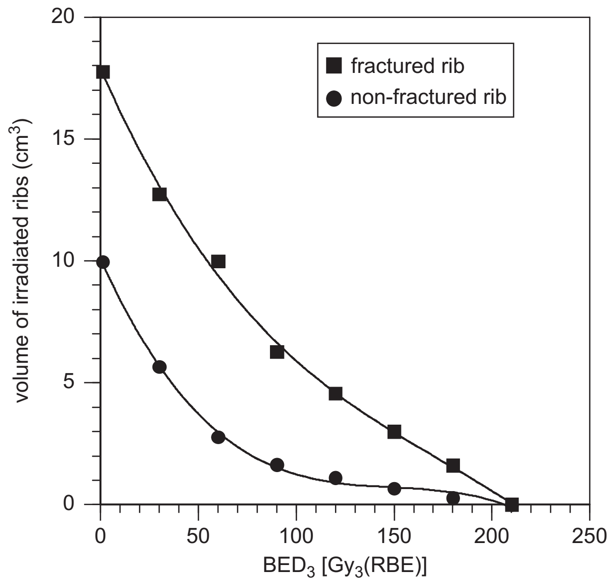

Figure 2. Mean irradiated rib volume and mean biologically effective dose (BED_3) to irradiated ribs. DVH parameters were all significantly higher in fractured ribs than in non-fractured ribs ($p < 0.05$).

Table I. The calculated areas under the curve of receiver operating characteristics curves and optimal cut-off point*.

	Calculated AUC	95% Confidence interval	Optimal cut-off point	The crude fracture rate above/below the cut-off point
V1	0.798	0.730–0.867	12.6 cm^3	21% / 2.0%
V30	0.822	0.762–0.882	9.80 cm^3	25% / 3.0%
V60	0.857	0.791–0.923	4.48 cm^3	26% / 1.4%
V90	0.837	0.763–0.911	3.10 cm^3	28% / 2.2%
V120	0.815	0.728–0.903	1.22 cm^3	26% / 2.6%
V150	0.798	0.701–0.895	0.21 cm^3	26% / 3.0%
V180	0.754	0.640–0.867	0.28 cm^3	35% / 3.8%
V210	0.519	0.401–0.636	0.09 cm^3	100% / 8.4%
D_{max}	0.854	0.784–0.925	150 Gy_3 (RBE)	25% / 2.7%
D_{1cm^3}	0.854	0.788–0.920	108 Gy_3 (RBE)	24% / 2.3%
D_{2cm^3}	0.852	0.790–0.914	96 Gy_3 (RBE)	25% / 2.2%
D_{5cm^3}	0.852	0.793–0.911	56 Gy_3 (RBE)	28% / 1.8%
D_{10cm^3}	0.830	0.757–0.904	20 Gy_3 (RBE)	23% / 2.7%

AUC, area under the curve; D_{max}, maximum dose for irradiated ribs; D_{Xcm^3}, doses received by irradiated rib volumes of X-cm^3; Vx, volume of rib receiving >x Gy_3 (RBE); *The doses Gy_3 (RBE) shown in this table denote biologically effective doses with 3 Gy (BED_3).

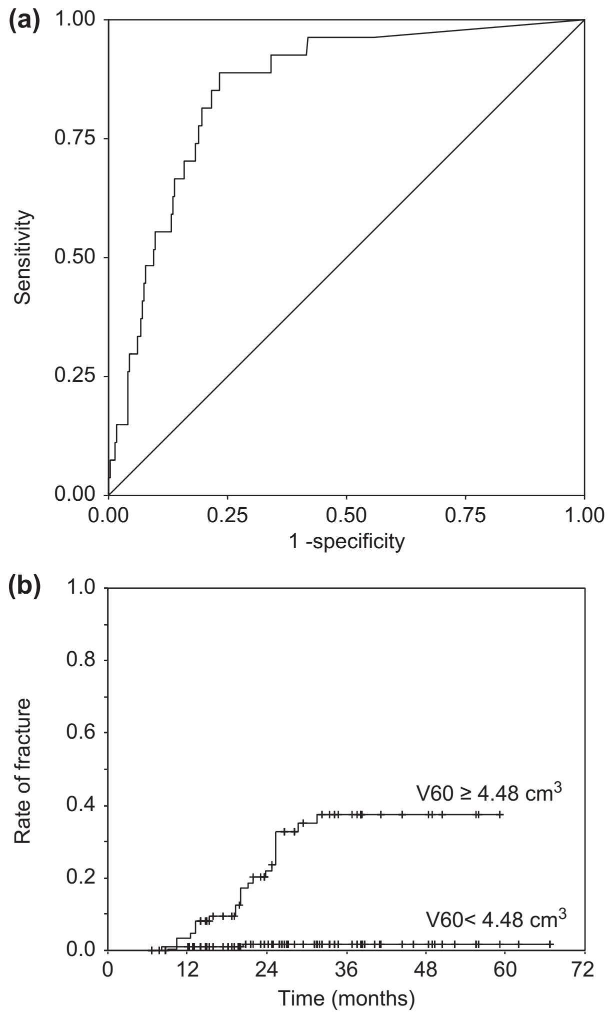

Figure 3. Receiver operating characteristics and rate of rib fracture at V60. (a) Among DVH parameters, the area under the curve was largest for V60. With receiver operating characteristics analysis at V60, the optimal cut-off point was 4.48 cm^3. The sensitivity of this point was 0.89 and the specificity was 0.77. (b) Curves of cumulative rates were significantly different between the irradiated volumes $<$4.48 cm^3 and volumes $\geq$4.48 cm^3 according to the log-rank test (p = 0.000).

function of volume of irradiated rib at V60 (Figure 4a), using the equation $p = 1/\{1 + \exp[-1 \times (-3.511 + 0.204 \times V60)]\}$. Using this logistic regression, 4.48 cm^3 was detected the value for 6.9% probability of

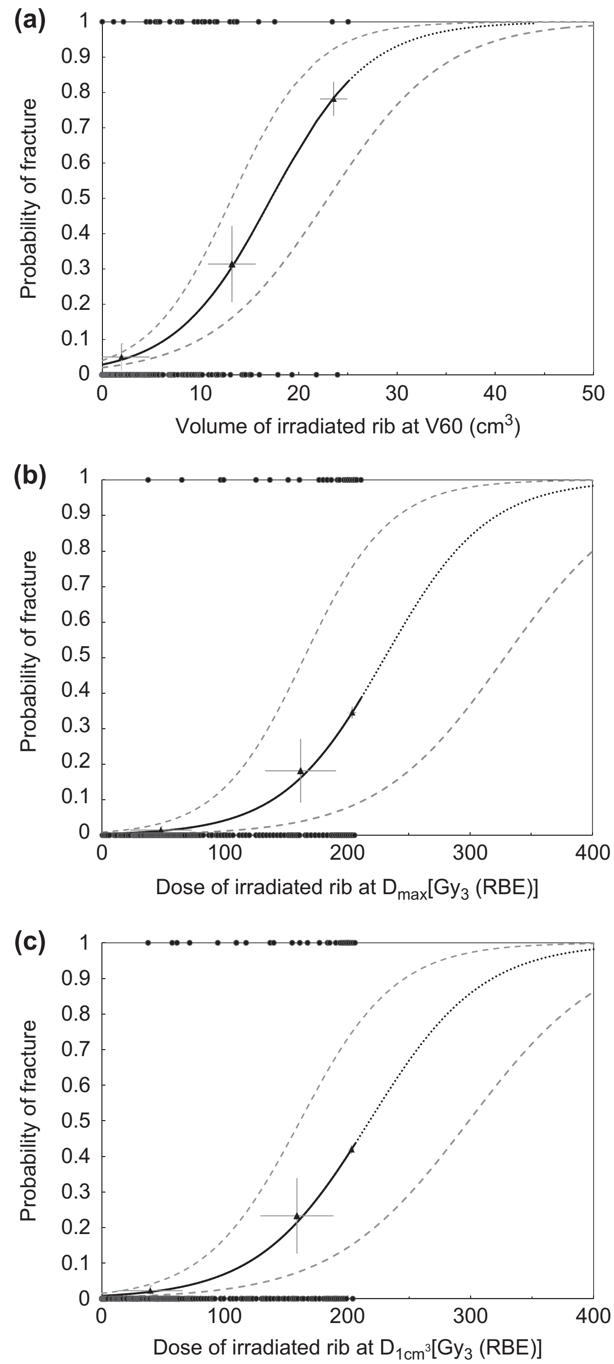

Figure 4. Volume-response curve at V60 (a) and dose-response curves at D_{max} (b) and D_{1cm^3} (c). Using logistic regression, each diagram (a)–(c) showed as following. The irradiated volume/dose points of each non-fractured or fractured rib were plotted on the lines y = 0 (non-fractured rib) or y = 1 (fractured rib) with circle both. The estimated volume- or dose-response curves within the range the x-values being observed are solid curve, but those exceeding the range are dotted one. The 68% confidence interval of each curve was drawn by dashed curve. The observed data was divided into three bins [according to each 10 cm^3 of V60 for diagram (a), each 100 Gy_3 (RBE) of D_{max} for diagram (b), and each 100 Gy_3 (RBE) of D_{1cm^3} for diagram (c)], and showed the mean (triangle point) and its standard deviation (SD) (mean ± SD was drawn by horizontal line segment) in each bin, respectively. Vertical line segment at each mean showed the 68% confidence interval for the observed probability calculated with binomial statistics. (a) Volume-response curve of the fracture proportion (p), a function of volume of irradiated rib at V60, was estimated by the equation $p = 1/\{1 + \exp[-1 \times (-3.511 + 0.204 \times V60)]\}$. The volume yielding 50% probability was 17.2 cm^3, and gamma 50 (representing the steepness of the curve at the point of 50% probability) was 0.88, respectively. b), c) Dose-response curves of the fracture rate (p), functions of dose of irradiated rib at D_{max} and $D_{1cm}3$, were generated using the regression $p = 1/\{1 + \exp[-1 \times (-5.535 + 0.024 \times D_{max})]\}$, and $p = 1/\{1 + \exp[-1 \times (-4.791 + 0.022 \times D_{1cm^3})]\}$, respectively. The doses that yields 50% probability / gamma 50 based on D_{max} and $D_{1cm}3$ were 231 Gy_3 (RBE) / 1.38 and 218 Gy_3 (RBE) / 1.20, respectively.

fracture. Dose-response curves for D_{max} and D_{1cm^3} were also shown in Figure 4b and c using logistic regression, respectively.

Discussion

Radiation-induced rib fracture is recognized as a late complication after external radiotherapy to the chest. Several factors associated with rib fracture must be considered, including dose, volume and site of irradiated rib, and patients' characteristics. In this study, no significant association with rib fracture was seen for sex, age, tumor size, tumor site, and follow-up period. By contrast, our DVH analysis of the 310 irradiated ribs showed that the irradiated volume and dose had significant effects on fracture rate. The DVH parameter most significantly associated with fracture was V60, which cut-off point of 4.48 cm^3 provided highest sensitivity and specificity. In addition, V30 to V120 and D_{max} to D_{10cm^3} were also considered to be clinically significant, because the AUCs of V30 to V120 and D_{max} to D_{10cm^3} were similar to that of V60.

To date, there are only a few reports on rib fracture after radiotherapy that have also examined irradiation doses and irradiated volumes of ribs in detail. Voroney et al. reported that the range of median dose to rib fracture site was 46–50 Gy in 3 fractions ($BED_3 = 281–328\ Gy_3$) [10]. Dunlap et al. reported that there was a 30% risk of developing severe chest wall pain for a 35-cm^3 volume of chest wall receiving 30 Gy in 3–5 fractions ($BED_3 = 90–130\ Gy_3$) [4]. Pettersson et al. reported the value for 5% and 50% probability of rib fracture with $D_{2cm^3} = 27.2$ Gy in 3 fractions ($BED_3 = 110\ Gy_3$) and 49.8 Gy in 3 fractions ($BED_3 = 325\ Gy_3$), respectively [8].

To allow comparison with Voroney's data [10], the median / average doses of D_{1cm^3}, D_{2cm^3}, D_{5cm^3}, and D_{10cm^3} for fractured rib were determined in our study. They were 192/171, 177/154, 161/142, 99/104, and 57/57 Gy_3, respectively. These results were all lower than the results of Voroney et al. To allow comparison with Pettersson's data [8], we also performed the logistic regression for D_{2cm^3}. The value for 5% probability of rib fracture at D_{2cm^3} was 110 Gy_3 (EQD2; 66 Gy_3) in Pettersson's study, whereas it was 74 Gy_3 (RBE) (EQD2; 44 Gy_3) determined using the equation $p = 1/\{1 + \exp[-1 \times (-4.488 + 0.021 \times D_{2cm^3})]\}$ in our study. The 74 Gy_3 (RBE) was a little lower than 110 Gy_3, which data were not perfectly consistent, but they were relatively close. Although it might be difficult to compare different hypofractionated radiotherapies and these studies' confidence intervals for dose-response curves were large, there was a positive association between rib fracture and irradiation dose in both studies.

The crude rate of fracture in our study was 16.4% of 67 patients and 8.7% of the 310 irradiated ribs in these 67 patients. Radiation-induced rib fracture has been commonly observed after conventional radiotherapy. Following breast-conserving radiotherapy at doses of 50 Gy in 25 fractions, the risk of rib fracture has been reported to be 0.3–3% [7,9]. Some studies have also reported fracture after hypofractionated radiotherapy with photons. The rate of rib fracture has been reported to be 2–21% after stereotactic body radiotherapy (SBRT) for lung cancer at doses of 24–60 Gy in 1–8 fractions [3–6,8,10,11]. After PBT for partial breast irradiation, Kozak et al. reported that three of 20 patients (15%) developed rib pain. These patients received 4 Gy (RBE) in 1 fraction, twice daily, over four days, with a total prescribed dose of 32 Gy (RBE) [25]. The morbidity rate in our study was higher than the previously reported rates after conventional radiotherapy and was similar to recent reports on morbidity of SBRT. Therefore, our DVH analysis may be considered useful for SBRT with photons.

In our study, the median interval for fracture occurrence in all patients was 25 months and also 25 months for all irradiated ribs. The interval from irradiation to rib fracture has been reported to range from 6 to 17 months in previous studies [4,10,11,25]. The interval reported previously and in our study showed quite a wide range. Our relationship analysis of DVH parameters and the interval determined that the p-values for D_{max} to D_{2cm^3} were not clearly significant, but they were close to significant (D_{max}, $p = 0.052$; D_{1cm^3}, $p = 0.059$; D_{2cm^3}, $p = 0.059$). This suggested that rib fracture possibly occurred early when D_{max} to D_{2cm^3} were large.

In conclusion, DVH parameters are useful for predicting late adverse events in ribs irradiated by PBT. This research determined that the volume of rib receiving a BED of more than 60 Gy_3 (RBE) (V60) (EQD2; 36 Gy_3), which cut-off point was 4.48 cm^3, was most statistically significant parameter. However, V30 to V120 (EQD2; 18–72 Gy_3) and D_{max} to D_{10cm^3} were also significant, and these parameters were considered to be clinically useful for estimating the risk of rib fracture after hypofractionated PBT.

Acknowledgements

Supported by institutional sources and in part by a Grant-in-Aid from the Ministry of Education, Science, Sports and Culture of Japan. None of the authors report any financial conflict regarding the work in the study.

Declaration of interest: The authors report no conflicts of interest. The authors alone are responsible for the content and writing of the paper.

References

[1] Papiez L, Timmerman R, DesRosiers C, Randall M. Extracranial stereotactic radioablation: Physical principles. Acta Oncol 2003;42:882–94.

[2] Potters L, Steinberg M, Rose C, Timmerman R, Ryu S, Hevezi JM, et al. American Society for Therapeutic Radiology and Oncology and American College of Radiology practice guideline for the performance of stereotactic body radiation therapy. Int J Radiat Oncol Biol Phys 2004; 60:1026–32.

[3] Baumann P, Nyman J, Lax I, Friesland S, Hoyer M, Rehn Ericsson S, et al. Factors important for efficacy of stereotactic body radiotherapy of medically inoperable stage I lung cancer. A retrospective analysis of patients treated in the Nordic countries. Acta Oncol 2006;45:787–95.

[4] Dunlap NE, Cai J, Biedermann GB, Yang W, Benedict SH, Sheng K, et al. Chest wall volume receiving > 30 Gy predicts risk of severe pain and/or rib fracture after lung stereotactic body radiotherapy. Int J Radiat Oncol Biol Phys 2010;76: 796–801.

[5] Fritz P, Kraus HJ, Blaschke T, Muhlnickel W, Strauch K, Engel-Riedel W, et al. Stereotactic, high single-dose irradiation of stage I non-small cell lung cancer (NSCLC) using four-dimensional CT scans for treatment planning. Lung Cancer 2008;60:193–9.

[6] Lagerwaard FJ, Haasbeek CJ, Smit EF, Slotman BJ, Senan S. Outcomes of risk-adapted fractionated stereotactic radiotherapy for stage I non-small-cell lung cancer. Int J Radiat Oncol Biol Phys 2008;70:685–92.

[7] Meric F, Buchholz TA, Mirza NQ, Vlastos G, Ames FC, Ross MI, et al. Long-term complications associated with breast-conservation surgery and radiotherapy. Ann Surg Oncol 2002;9:543–9.

[8] Pettersson N, Nyman J, Johansson KA. Radiation-induced rib fractures after hypofractionated stereotactic body radiation therapy of non-small cell lung cancer: A dose- and volume-response analysis. Radiother Oncol 2009;91:360–8.

[9] Stotter AT, McNeese MD, Ames FC, Oswald MJ, Ellerbroek NA. Predicting the rate and extent of locoregional failure after breast conservation therapy for early breast cancer. Cancer 1989;64:2217–25.

[10] Voroney JP, Hope A, Dahele MR, Purdie TG, Franks KN, Pearson S, et al. Chest wall pain and rib fracture after stereotactic radiotherapy for peripheral non-small cell lung cancer. J Thorac Oncol 2009;4:1035–7.

[11] Zimmermann FB, Geinitz H, Schill S, Thamm R, Nieder C, Schratzenstaller U, et al. Stereotactic hypofractionated radiotherapy in stage I (T1-2 N0 M0) non-small-cell lung cancer (NSCLC). Acta Oncol 2006;45:796–801.

[12] Nirula R, Mayberry JC. Rib fracture fixation: Controversies and technical challenges. Am Surg 2010;76:793–802.

[13] Bush DA, Hillebrand DJ, Slater JM, Slater JD. High-dose proton beam radiotherapy of hepatocellular carcinoma: Preliminary results of a phase II trial. Gastroenterology 2004;127:S189–93.

[14] Chiba T, Tokuuye K, Matsuzaki Y, Sugahara S, Chuganji Y, Kagei K, et al. Proton beam therapy for hepatocellular carcinoma: A retrospective review of 162 patients. Clin Cancer Res 2005;11:3799–805.

[15] Fukumitsu N, Sugahara S, Nakayama H, Fukuda K, Mizumoto M, Abei M, et al. A prospective study of hypofractionated proton beam therapy for patients with hepatocellular carcinoma. Int J Radiat Oncol Biol Phys 2009; 74:831–6.

[16] Mizumoto M, Okumura T, Hashimoto T, Fukuda K, Ochiro Y, Fukumitsu N, et al. Proton beam therapy for hepatocellular carcinoma: A comparison of three treatment protocols. Int J Radiat Oncol Biol Phys 2011;81:1039–45.

[17] Bush DA, Kayali Z, Grove R, Slater JD. The safety and efficacy of high-dose proton beam radiotherapy for hepatocellular carcinoma: A phase 2 prospective trial. Cancer 2011; 117:3053–9.

[18] Kawashima M, Kohno R, Nakachi K, Nishio T, Mitsunaga S, Ikeda M, et al. Dose-volume histogram analysis of the safety of proton beam therapy for unresectable hepatocellular carcinoma. Int J Radiat Oncol Biol Phys 2011; 79:1479–86.

[19] Mizumoto M, Tokuuye K, Sugahara S, Nakayama H, Fukumitsu N, Ohara K, et al. Proton beam therapy for hepatocellular carcinoma adjacent to the porta hepatis. Int J Radiat Oncol Biol Phys 2008;71:462–7.

[20] Paganetti H, Niemierko A, Ancukiewicz M, Gerweck LE, Goitein M, Loeffler JS, et al. Relative biological effectiveness (RBE) values for proton beam therapy. Int J Radiat Oncol Biol Phys 2002;53:407–21.

[21] Fowler JF. The linear-quadratic formula and progress in fractionated radiotherapy. Br J Radiol 1989;62:679–94.

[22] Tsunashima Y, Sakae T, Shioyama Y, Kagei K, Terunuma T, Nohtomi A, et al. Correlation between the respiratory waveform measured using a respiratory sensor and 3D tumor motion in gated radiotherapy. Int J Radiat Oncol Biol Phys 2004;60:951–8.

[23] Kaplan EL, Meier P. Nonparametric estimation from incomplete observations. J Am Stat Assoc 1958;53:457–81.

[24] Akobeng AK. Understanding diagnostic tests 3: Receiver operating characteristic curves. Acta Paediatr 2007;96:644–7.

[25] Kozak KR, Smith BL, Adams J, Kornmehl E, Katz A, Gradd M, et al. Accelerated partial-breast irradiation using proton beams: Initial clinical experience. Int J Radiat Oncol Biol Phys 2006;66:691–8.